

A molecular dynamics simulation study of hydrogen bonding in aqueous ionic solutions

Elvira Guàrdia^{a,*}, Jordi Martí^a, Lino García-Tarrés^a, Daniel Laria^{b,c}

^aDepartament de Física i Enginyeria Nuclear, Universitat Politècnica de Catalunya, B4–B5 Campus Nord, Jordi Girona 1–3, 08034 Barcelona, Spain

^bUnidad Actividad Química, Comisión Nacional de Energía Atómica, Av. del Libertador 8250, 1429 Buenos Aires, Argentina

^cDepartamento de Química Inorgánica, Analítica y Química Física, Facultad de Ciencias Exactas y Naturales, Universidad de Buenos Aires, Pabellón II, 1428 Buenos Aires, Argentina

Available online 25 September 2004

Abstract

A series of molecular dynamics (MD) simulations have been carried out to study hydrogen bonding in aqueous ionic solutions at ambient conditions. Alkali metal and halides with different sizes have been considered. A separate study of the hydrogen bond (HB) populations in the first and second hydration shells has been performed and characteristic lifetimes of the hydrogen bonds have been determined in each case. The influence of ion size and charge is discussed.

© 2004 Elsevier B.V. All rights reserved.

Keywords: Molecular dynamics simulation; Hydrogen bonding; Aqueous ionic solution

1. Introduction

The origin of many properties that make liquid water a unique fluid in nature can be traced back to its microscopic hydrogen bond (HB) structure [1,2]. Hydrogen bond distributions and the rates of HB breaking and reformation drive microscopic water dynamics in the sub-picosecond time scale. The presence of ionic species can produce important perturbations of both the structure and dynamics of water through changes in the behavior of the HB network. Molecular dynamics (MD) simulations provide direct information about the HB structure and dynamics at the microscopic level. Over the past decade, several MD studies of hydrogen bonding in pure water at different thermodynamic conditions have been published [3–11]. More recently, these kinds of studies have been extended to aqueous electrolyte solutions at room temperature [12–14]. However, the ion-induced

modifications of the HB properties are far from being fully understood. The present work is aimed to make a further contribution in this direction. As a difference with previous works, we have performed a separate study of the HB populations and lifetimes in the first and second hydration shells for different ionic species, and the influence of ion size and charge has been systematically investigated.

2. Computer simulation details

We carried out MD simulations on a system containing one ion and 255 water molecules with periodic boundary conditions. Three alkali metal (Li^+ , Na^+ , Cs^+) and three halides (F^- , Cl^- , I^-) species were considered. In each case, the size of the cubic box was chosen to give a solvent density $\rho=1 \text{ g cm}^{-3}$ and the temperature was kept at $T=298 \text{ K}$. The SPC/E model was adopted for water–water interactions [15]. This is a three-site water model which has been widely used for pure water as well as for aqueous ionic solutions. The ion–water forces were modeled by means of a sum of pairwise additive Coulombic and 6–12

* Corresponding author.

E-mail address: elvira.guardia@upc.es (E. Guàrdia).

Table 1
Interaction potential parameters

Ion/atom	ϵ (kcal/mol)	σ (Å)	q (e)	Reference
Li ⁺	0.165	1.506	+1.0	[16]
Na ⁺	0.100	2.584	+1.0	[17]
Cs ⁺	0.100	3.884	+1.0	[17]
F ⁻	0.180	3.117	-1.0	[18]
Cl ⁻	0.100	4.401	-1.0	[17]
I ⁻	0.100	5.167	-1.0	[19]
Oxygen	0.155	3.166	-0.8476	[15]
Hydrogen			+0.4236	[15]

Lennard–Jones site–site potentials. The Lorentz–Berthelot mixing rules, i.e., $\epsilon_{ij} = \sqrt{\epsilon_i \epsilon_j}$ and $\sigma_{ij} = (\sigma_i + \sigma_j)/2$, were assumed. We adopted the set of ion Lennard–Jones

parameters derived by Dang et al. [16–19]. All the potential parameters are collected in Table 1.

To carry out the simulations, we employed the integration algorithm of Berendsen et al. [20] with a time step of 0.002 ps and a thermal bath coupling parameter of 0.2 ps. Short-ranged forces were truncated at half the box length and the Ewald summation method with conducting boundary conditions [21] was applied to account for long-range Coulomb interactions. Each run consisted of an initial equilibration period of 50 ps and a production period of 250 ps to collect statistically meaningful properties. An auxiliary simulation of pure water under identical conditions was also carried out. In this case, the simulation length was 100 ps.

3. H bond definition and H bond lifetimes

We assumed that two water molecules are H bonded if three geometrical conditions are fulfilled:

- (1) The distance R_{OO} between the oxygens is lower than R_{OO}^c ,
- (2) The distance R_{OH} between the “acceptor” oxygen and the hydrogen of the “donor” molecule is lower than R_{OH}^c ,
- (3) The H–O...O angle φ is lower than φ^c .

In all our simulations, the assumed cutoff distances were $R_{OO}^c = 3.4$ Å and $R_{OH}^c = 2.425$ Å. These cutoff values correspond to the positions of the first minimum of the oxygen–oxygen and hydrogen–oxygen radial distribution functions for pure SPC/E water at ambient conditions. The angular cutoff was chosen to be $\varphi^c = 30^\circ$. This is a choice widely accepted in the literature (see, for instance, Ref. [4]).

The analysis of the dynamics of the HB network was performed through the calculation of the HB lifetimes. We obtained the survival probability or lifetime of the H bonds from the long time decay of the autocorrelation functions [22]

$$C_{HB}(t) = \frac{\langle \eta_{ij}(t) \eta_{ij}(0) \rangle}{\langle \eta_{ij}(0)^2 \rangle} \cong \exp \left\{ -\frac{t}{\tau_{HB}} \right\} \text{ (at long times)} \quad (1)$$

where the variable $\eta_{ij}(t)$ takes the values 0 or 1 depending on the H bond state of a given pair of molecules:

$$\eta_{ij}(t) = \begin{cases} 1, & \text{if molecules } i \text{ and } j \text{ are H bonded at times } 0 \text{ and } t \text{ and the bond has not been broken for any period longer than } t^* \\ 0, & \text{otherwise} \end{cases} \quad (2)$$

This procedure is similar to that proposed by Rapaport [23] and Matsumoto and Gubbins [24]. The limiting cases $t^* = 0$ and $t^* = \infty$ correspond to the so-called continuous (τ_{HB}^C) and intermittent (τ_{HB}^I) H bond lifetimes, respectively [23].

4. Results and discussion

In order to examine the characteristics of hydrogen bonding in the close vicinity of the different ionic species, we separately considered the modifications that operate in the first and in the second hydration shells. The boundaries of these shells were defined by the positions of the first and second minima of the ion–oxygen radial distribution functions displayed in Fig. 1. In all cases, the position of the first minimum is well defined; some ambiguity was found in the position of the second minimum for Cs⁺, which we assumed to be located at 6 Å.

4.1. HB statistics

Distributions of HB populations were characterized by computing the fraction f_n of molecules lying within a given hydration shell which exhibit n H bonds. In addition, the average numbers of HB per molecule n_{HB} were also computed. Results for f_n are presented in Figs. 2 and 3. The n_{HB} values are collected in Table 2. In the first ionic hydration shell, the differences with respect to the pure water reference values are most remarkable. In the close vicinity of the ions (see Fig. 2), f_1 and f_2 decrease with ionic size, whereas f_3 and f_4 show the opposite trend. These effects are especially evident in the case of alkali metal ions. The HB

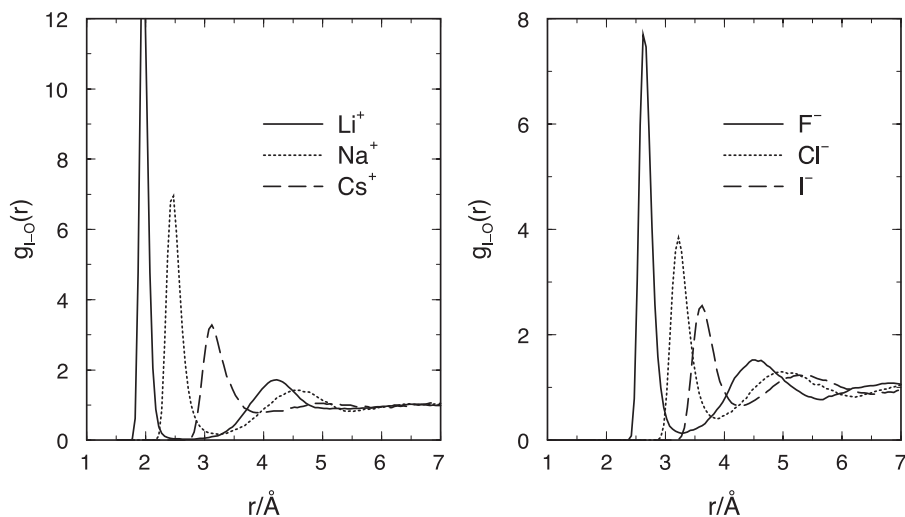


Fig. 1. Ion-oxygen radial distribution functions for alkali metal (left) and halides (right) at $T=298$ K and $\rho=1$ g cm⁻³.

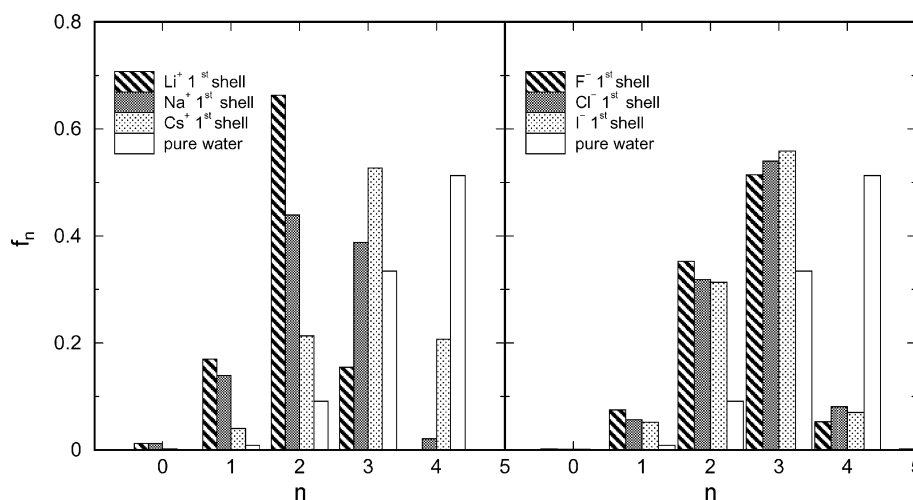


Fig. 2. Fraction f_n of molecules with n H bonds in the first hydration shell of different alkali metal (left) and halide (right) ions. f_n values corresponding to pure water are also depicted.

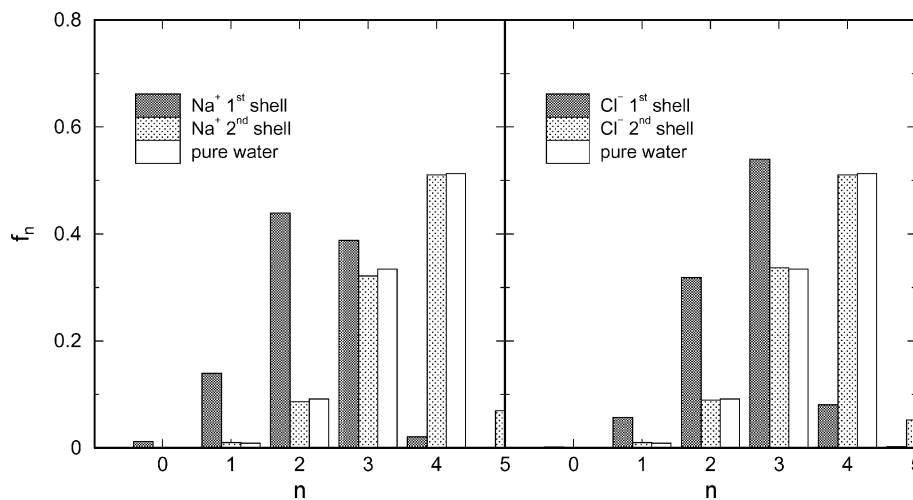


Fig. 3. Fraction f_n of molecules with n H bonds in the first and second hydration shells of Na⁺ (left) and Cl⁻ (right). f_n values corresponding to pure water are also depicted.

Table 2

Mean number of H bonds per molecule and H bond lifetimes in the first and second hydration shells of different alkali metal and halide ions

Ion	n_{HB}		$\tau_{\text{HB}}^{\text{C}}$		$\tau_{\text{HB}}^{\text{I}}$	
	First shell	Second shell	First shell	Second shell	First shell	Second shell
Li ⁺	1.97	3.52	0.71 (0.53)	0.68 (0.54)	5.8 (4.6)	6.1 (4.8)
Na ⁺	2.27	3.55	0.63 (0.46)	0.70 (0.53)	5.7 (4.2)	6.1 (4.7)
Cs ⁺	2.92	3.56	0.71 (0.56)	0.69 (0.55)	5.7 (4.6)	6.0 (4.8)
F ⁻	2.54	3.53	0.76 (0.60)	0.71 (0.56)	7.2 (5.6)	6.6 (5.2)
Cl ⁻	2.65	3.51	0.72 (0.58)	0.71 (0.57)	6.4 (5.1)	6.0 (4.8)
I ⁻	2.65	3.50	0.73 (0.59)	0.70 (0.57)	5.9 (4.9)	5.9 (4.8)
Pure water		3.51		0.70 (0.55)		5.0 (4.1)

n_{HB} and τ_{HB} corresponding to pure water are also included. Quantities in parenthesis are the time integrals of $C_{\text{HB}}(t)$.

distribution in the vicinity of Li⁺ is mainly dominated by water molecules forming two HB. For the Na⁺ ion, we observe that the most probable populations involve molecules exhibiting two and three HB, whereas for Cs⁺, the main population corresponds to molecules with three HB, with a noticeable contribution of the four HB type as well. Therefore, as ionic size increases, the HB distributions look more similar to the pure water case. A similar trend is observed when comparing HB distributions in the first hydration shell of different halide ions. However, it must be remarked that in this case, independently of the ionic size, the most probable populations correspond to molecules exhibiting three HB. Conversely, the situation in the second hydration shell remains basically identical to that of pure water, regardless of the charge and size of the ionic solutes. This is explicitly shown in Fig. 3 for the case of Na⁺ and Cl⁻. In accordance with the previous discussion, the mean number of HB per molecule (see Table 2) diminishes due to the presence of the ions. This effect is more important in

the case of small positively charged ions. Finally, as we can also see in Table 2, n_{HB} values corresponding to molecules lying in the second hydration shell are identical to that of pure water in all cases.

4.2. HB lifetimes

Our results show that the overall hydrogen bond dynamics in ionic solutions is slower than in pure water. Plots for the continuous ($C_{\text{HB}}^{\text{C}}(t)$) and intermittent ($C_{\text{HB}}^{\text{I}}(t)$) HB autocorrelation functions are displayed in Fig. 4, where the contributions from water molecules from the first and second ionic hydration shells of F⁻ have been separately considered and compared to the ones corresponding to the pure water system. The influence of the ion is much more important for $C_{\text{HB}}^{\text{I}}(t)$ than for $C_{\text{HB}}^{\text{C}}(t)$. Moreover, in the case of the intermittent $C_{\text{HB}}^{\text{I}}(t)$ function, this influence extends out the first hydration shell and significantly affects the molecules lying in the second hydration shell. Similar

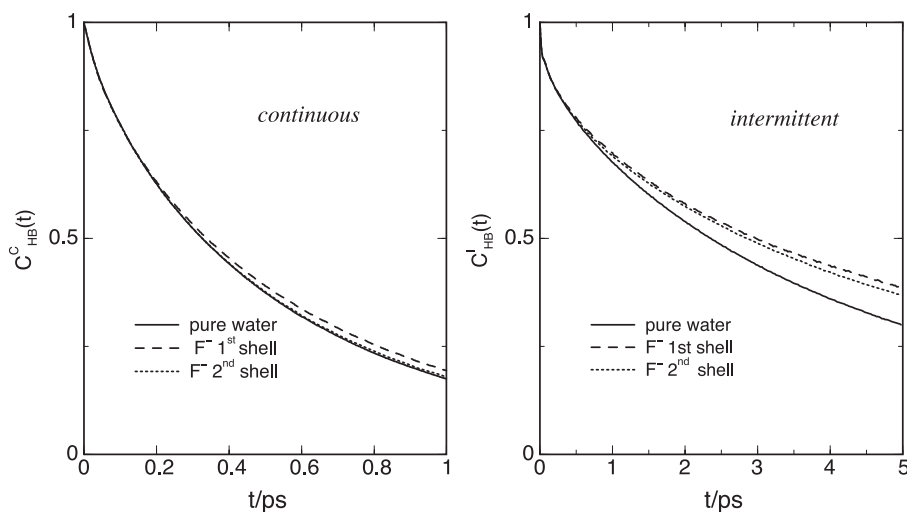


Fig. 4. Continuous (left) and intermittent (right) HB autocorrelation functions for molecules lying in the first and second hydration shells of F⁻. $C_{\text{HB}}^{\text{C}}(t)$ and $C_{\text{HB}}^{\text{I}}(t)$ values corresponding to pure water are also depicted.

features are observed when analyzing the HB autocorrelation functions corresponding to the hydration molecules of the different ionic species.

The computed HB lifetimes are listed in Table 2 for all the alkali metal and halide ions. For the sake of completeness, the time integrals of $C_{\text{HB}}^{\text{C}}(t)$ and $C_{\text{HB}}^{\text{I}}(t)$ are also given. In general, the continuous $\tau_{\text{HB}}^{\text{C}}$ lifetimes of water molecules in both the first and second hydration shells are similar to the one of pure water. The more significant deviations (up to 10%) are observed in the first hydration shells of Na^+ and F^- . On the contrary, the intermittent $\tau_{\text{HB}}^{\text{I}}$ lifetime increases between 20% and 40% due to the presence of the ions. The ionic size of alkali metal species do not affects significantly the HB lifetimes. In the case of halides, we observe a systematic increase of both $\tau_{\text{HB}}^{\text{C}}$ and $\tau_{\text{HB}}^{\text{I}}$ with decreasing ion size, with the slowest decay times associated to the smallest species (F^-). For all the ionic species, HB lifetimes corresponding to the first and second hydration shell molecules are very similar.

5. Summary

We report the results of a series of MD simulations of alkali metal and halide ions in water at ambient conditions using the SPC/E model for water–water interactions. We have focussed our attention on the analysis of the hydrogen bond populations and lifetimes. Concerning HB populations, we found that the most remarkable differences with respect to the pure water tetrahedral network are observed when one examines water molecules located in the first ionic hydration shell. HB lifetimes have been computed and compared to the values of pure water. In all cases, the so-called continuous HB lifetime is very similar to the one obtained for pure water, whereas the intermittent HB lifetime systematically increases due to the presence of the ions. We observed a similar influence of the ions on the hydrogen bond dynamics of both the first and second hydration shell molecules.

Acknowledgments

The authors gratefully acknowledge financial support from the Secretaría de Educación y Universidades de España, the Direcció General de Recerca de la Generalitat de Catalunya (Grant 2001SGR-00222) and the Ministerio de Ciencia y Tecnología de España (Grant BFM2003-08211-C03-01). DL is a member of Carrera del Investigador Científico de CONICET (Argentina).

References

- [1] D. Eisenberg, W. Kauzmann, *The Structure and Properties of Water*, Oxford University Press, New York, 1969.
- [2] F. Franks (Ed.), *Water: A Comprehensive Treatise*, Plenum Press, New York, 1972.
- [3] F. Sciortino, A. Geiger, H.E. Stanley, *J. Chem. Phys.* 96 (1992) 3857.
- [4] A. Luzar, D. Chandler, *J. Chem. Phys.* 98 (1993) 8160.
- [5] T.I. Mizan, P.E. Savage, R.M. Ziff, *J. Phys. Chem.* 100 (1996) 403.
- [6] J. Martí, J.A. Padró, E. Guàrdia, *J. Chem. Phys.* 105 (1996) 639.
- [7] F. Csajka, D. Chandler, *J. Chem. Phys.* 109 (1998) 1125.
- [8] F.W. Starr, J.K. Nielsen, H.E. Stanley, *Phys. Rev. Lett.* 92 (1999) 3857.
- [9] J. Martí, *J. Chem. Phys.* 110 (1999) 6876.
- [10] A. Luzar, *J. Chem. Phys.* 113 (2000) 10663.
- [11] J. Martí, *Phys. Rev.*, E 61 (2000) 449.
- [12] T. Długoborski, E. Hawlicka, D. Swiatla-Wojcik, *J. Mol. Liq.* 85 (2000) 97.
- [13] A. Chandra, *Phys. Rev. Lett.* 85 (2000) 768.
- [14] A. Chandra, S. Chowdhuri, *J. Phys. Chem.*, B 106 (2002) 6779.
- [15] H.J.C. Berendsen, J.R. Grigera, T.P. Straatsma, *J. Phys. Chem.* 91 (1987) 6269.
- [16] L.X. Dang, *J. Chem. Phys.* 96 (1992) 6970.
- [17] L.X. Dang, *J. Am. Chem. Soc.* 117 (1995) 6954.
- [18] L.X. Dang, *Chem. Phys. Lett.* 200 (1992) 21.
- [19] L.X. Dang, B.C. Garrett, *J. Chem. Phys.* 99 (1993) 2972.
- [20] H.J.C. Berendsen, J.P.M. Postma, W.F. van Gunsteren, A. DiNola, J.R. Haak, *J. Phys. Chem.* 81 (1984) 3684.
- [21] M.P. Allen, D.J. Tildesley, *Computer Simulation of Liquids*, Clarendon Press, Oxford, 1987, Chap. 5.
- [22] J.A. Padró, L. Saiz, E. Guàrdia, *J. Mol. Struct.* 416 (1997) 243.
- [23] D.C. Rapaport, *Mol. Phys.* 50 (1983) 1151.
- [24] M. Matsumoto, K.E. Gubbins, *J. Chem. Phys.* 93 (1990) 1981.